

Heidi Jensen

Winter operations of permeable interlocking concrete pavement

Master's thesis in Civil and Environmental Engineering

Supervisor: Tone Merete Muthanna and Edvard Sivertsen

January 2020

NTNU
Norwegian University of Science and Technology
Faculty of Engineering
Department of Civil and Environmental Engineering



Norwegian University of
Science and Technology

Heidi Jensen

Winter operations of permeable interlocking concrete pavement

Master's thesis in Civil and Environmental Engineering
Supervisor: Tone Merete Muthanna and Edvard Sivertsen
January 2020

Norwegian University of Science and Technology
Faculty of Engineering
Department of Civil and Environmental Engineering



Description of Master Thesis Autumn 2019

Candidate name: Heidi Jensen

Subject: Stormwater

Title: Winter operation of permeable interlocking concrete pavement

Start date: September 4th 2019

Due date: January 29th 2020

Background

Heavy urbanization and precipitation intensities are adding pressure to existing stormwater systems. Consequently, many systems need upgrades that counteract these effects and at the same time also take into account the expected future rainfall extremes caused by climate change. In Norway, policies and practice focus on solutions that are open and local as alternative to traditional piped systems. Permeable interlocking concrete pavement is one such solution that can manage the stormwater locally and at the same time offer a hard surface useful for parking areas and roads.

The permeable interlocking concrete pavement infiltrate the stormwater to the ground through slits between the concrete stones. The slits are filled with gravel, that in most cases determine the infiltration capacity of the solution. As small particles will give low infiltration capacity, filling with grading 2-5 *mm* is normally used to ensure sufficient infiltration capacity. Hence, permeable interlocking concrete pavement is vulnerable to dust and other particles that may be present in an urban environment. Of special concern is the effect of sand put on ice/snow during the winter season to enhance the friction of the roads.

The effect of fine particles from winter operation of roads on the infiltration capacity will be investigated in laboratory column tests. Selected conditions will be further tested in a small pilot of a complete permeable interlocking concrete pavement, i.e. concrete stone, gravel filling, fine layer, support layer, layer representing the soil. The pilot tests will use the "climate lab" to test the effect of climate-related variables such as thawing / freezing cycles. For both the laboratory and pilot tests a suitable experimental procedure will be developed.

Research questions

The objective of this research is to investigate what effect winter operation of roads has on permeable interlocking concrete pavement and propose countermeasures to avoid reduction in the stormwater management capacity over time. The master thesis aims to answer the following research questions:

1. Do the sediments of crushed sand influence the infiltration capacity of the gravel fillings in the slits?
2. To what extent represent the current practice of using sand during winter operation a problem to permeable interlocking concrete pavements?

Collaboration partners: BIA-project Drensstein and Klima2050

Location: The master thesis will be conducted at the Department of Civil and Environmental Engineering and at the Klimalab at SINTEF Community. The candidate should have regular meetings with advisor(s). The simulations and models will be used with licenses and software available at the Department of Civil and Environmental Engineering

Advisors: Tone Merete Muthanna, Edvard Sivertsen

Abstract

The combination of climate change and urbanization leads to problems with handling the increasing stormwater volumes and faster peak flows. The traditional way of handling stormwater through pipelines to the recipient does not have sufficient capacity. Therefore, a less traditional way of handling stormwater utilizing the infiltration and storage capacity of semi-natural devices, like raingardens, swales, green roofs and permeable pavement increases in popularity.

In Norway there have been little use of permeable pavement, often due to uncertainty related to both the hydraulic and structural functionality in cold climate and with normal winter operations of roads with sand, salt or a combination used as a friction agent. There is a knowledge gap related to how the use of gritting sand influences the infiltration capacity of permeable interlocking concrete pavement which this master thesis will contribute to filling this gap.

A column test was performed on joint material containing different fractions of crushed rock grading 0-2 *mm* to measure the saturated hydraulic conductivity to measure the effect of the crushed rock. Crushed rock was used as a substitution of used gritting sand due to it being impossible to obtain used gritting sand during the fall. The biggest decrease in the saturated hydraulic conductivity was observed when the fraction of crushed rock increases from 25 % to 50 %, resulting in a decrease of 93 % from 2.97 *mm/s* to 0.21 *mm/s*.

Further a small-scale pilot of a permeable interlocking concrete was constructed, to see if the results from the column test could be observed on a larger scale. The pilot was performed in a climate room since the effect of cold temperature is interesting. The plan was to perform a falling head test to measure the hydraulic conductivity of the pavement. Using the planned method that was not possible, due to water to fast to gain an initial water level. Instead the outflow rate from a pilot with pure joint material, and a pilot with 50 % crushed rock in the joint material was compared. Here no reduction in outflow rate was observed for the one with 50 % crushed rock.

Sammendrag

Kombinasjonen av klimaforandringer og urbanisering har ført til problemer med å håndtere det økende volumet av overvann og at den maksimale vannføringen skjer tidligere. Tradisjonelt har overvann blitt ført til resipienten via ledninger, som ikke lengre har nødvendig kapasitet. En mindre tradisjonell måte å håndtere overvannet gjennom å utnytte infiltrasjons- og lagringskapasiteten til naturinspirerte, som regnbed, vadier, grønne tak og permeable dekker, har dermed økt i popularitet.

I Norge har bruken av permeabelt dekke vært liten, ofte grunnet usikkerheten knyttet til både den hydrauliske- og strukturelle funksjonaliteten i kaldt klima og med den normale vinterdriften av veier med strøsand, salt eller en kombinasjon, brukt for å øke friksjonen. Det er et kunnskapshull knyttet til hvordan bruken av strøsand påvirker infiltrasjonskapasiteten til belegningsstein med permeable fuger, og dette masteren vil bidra til å tette dette kunnskapshullet.

En kolonnetest utført på fugematerialet med forskjellige andeler knust stein med gradering 0-2 mm for å måle den mettede hydrauliske konduktiviteten, for å måle effekten av knust stein. Knust stein ble brukt som en erstatning brukt strøsand, siden det var umulig å skaffe brukt strøsand om høsten. Den største reduksjonen i den mettede hydrauliske konduktiviteten ble målt når fraksjonen av knust stein økte fra 25 % til 50 %, da den ble redusert med 93 % fra 2.97 mm/s til 0.21 mm/s.

Videre ble det konstruert et pilotforsøk med et permeabelt dekke for å se om resultatene fra kolonnetesten kunne observeres i større skala. Pilotforsøket ble utført i et klimarom, siden effekten av lav temperatur er interessant. Planen var å utføre en fallende hode-test for å måle den hydrauliske konduktiviteten til dekket. Den planlagte metoden var ikke mulig å bruke, siden vannet ble infiltrert for raskt til å oppnå stående vann på belegningssteinen. Istedenfor ble vannføringen ut av dekket med 50 % knust stein i fugemassen sammenlignet med vannføringen ut av dekket med ren fugemasse. Her ble det ikke observert noen reduksjon i vannføringen for forsøket med 50 % knust stein i fugemassen.

Preface

This master thesis is the final product of the course "TVM4905 Water and wastewater engineering, Master's thesis" at the Norwegian University of Science and Technology (NTNU). The thesis is written during the autumn semester 2019, the final semester at the Water and Wastewater Division and Department of Civil and Environmental Engineering. The work was carried out September 2019 to January 2020 and includes a grain size distribution test, five column tests and two small-scale pilot experiments.

The thesis has an untraditional format with a scientific paper as a main product. This decision was made in agreement with supervisors Tone Merete Muthanna and Edvard Sivertsen. Additional information about the work, not written in the paper, is found in Appendix A-B. An outline paper has been submitted to the International Water Association World Water Congress & Exhibition 2020. The work was also presented at Tekna kursdagene: Sustainability in the water industry- Stormwater, in January 2020.

The research was founded by the User-driven Research based Innovation (BIA)-project Drensstein.

I would like to thank both my supervisors Tone Merete Muthanna, associate professor at NTNU, and Edvard Sivertsen, Senior Research Scientist at SINTEF, for good help during the work with this master thesis. I would also like to thank Egil Rognvik, senior engineer at SINTEF, for help and good ideas with pilot and Asbjørn Rafdal for constructing the box used for the pilot in his master thesis. In addition, I would like to thank Endre Våland Bø for help with setting up the datalogger used for the moisture sensors. At last I would like to thank my family and friends for support during the whole degree.

Contents

- Figures..... xii
- Tables xiii
- 1 Introduction..... 1
- 2 Materials and method 4
 - 2.1 Materials 4
 - 2.2 Methods 4
 - 2.2.1 Grain size distribution 4
 - 2.2.2 Column tests 5
 - 2.2.3 Small scale pilot test 9
- 3 Results and Discussion15
 - 3.1 Grain size distribution15
 - 3.2 Column tests16
 - 3.3 Pilot test18
- 4 Conclusion20
- 5 Further work.....21
- References22
- Appendices I
 - A. Column test I
 - B. Pilot test IV

Figures

Figure 1: Illustration of the setup for the column test.....	7
Figure 2: Picture of the setup for the column test. Photo: Heidi Jensen.....	8
Figure 3: Construction of the permeable interlocking concrete pavement for the pilot with placement of the temperature sensors.	10
Figure 4: Figure showing the placement of the Divers, humidity and soil moisture sensors in the horizontal plan.	12
Figure 5: Picture showing how the joint material have been liftet from the slits during the first test Photo: Heidi Jensen	13
Figure 6: Picture showing the setup with the wooden board for test 2. Photo: Heidi Jensen	14
Figure 7: Grain size distribution for the crushed rock.	16
Figure 8: The plot shows how the saturated hydraulic conductivity varies with the fraction of crushed stone in the joint material.	17
Figure 9: Graph showing the effluent flow based on the water level measured by the to Divers in the effluent box for both experiments.	18
Figure 10: Graph showing the measurements from the humidity sensor 40 cm from the bottom during pilot test 1.	IV
Figure 11: Graph showing the measurements from the humidity sensor 30 cm from the bottom during pilot test 1.	IV
Figure 12: Graph showing the measurements from the humidity sensor 20 cm from the bottom during pilot test 1.	V
Figure 13: Graph showing the measurements from the humidity sensor 10 cm from the bottom during pilot test 1.	V
Figure 14: Graph showing the measurements from the humidity sensor 40 cm from the bottom during pilot test 2.	V
Figure 15: Graph showing the measurements from the humidity sensor 30 cm from the bottom during pilot test 2.	VI
Figure 16: Graph showing the measurements from the humidity sensor 20 cm from the bottom during pilot test 2.	VI
Figure 17: Graph showing the measurements from the humidity sensor 10 cm from the bottom during pilot test 2.	VI
Figure 18: Temperature development in the pavement from 13/12/2019 until air temperature is turned up during pilot test 1.	VII
Figure 19: Temperature development in the pavement from the air temperature was turned up during pilot test 1.	VIII
Figure 20: Temperature development in the pavement until air temperature is turned up during pilot test 2.	IX
Figure 21: Temperature development in the pavement from the air temperature was turned up during pilot test 2.	X

Tables

Table 1: Shows the setup of the column tests with the weight percent of joint material and crushed rock and the total weight of the material for each test and the measuring time used for each test.	6
Table 2: The instrumentation of the pilot	11
Table 3: Results from the sieving analysis with weight of remaining material on each sieve and the fraction of total mass passing the sieves.....	15
Table 4: Effluent water volume for test 1.....	I
Table 5: Effluent water volume for test 2.....	I
Table 6: Effluent water volume for test 3.....	II
Table 7: Effluent water volume for test 4.....	II
Table 8: Effluent water volume for test 5.....	II
Table 9: Variables used in Darcy's formula to calculate the saturated hydraulic conductivity.	III
Table 10: Saturated hydraulic conductivity for all three columns for each test and the average value for the tests.	III

Heidi Jensen

Norwegian University of Science and Technology, 2020

Abstract: Climate change and urbanization are leading to increased rain intensities and subsequent increased runoff, which increases the pressure on the existing drainage systems. Permeable interlocking concrete pavement (PICP) is a stormwater measure that can contribute to reducing this pressure. Particles and sediment can reduce the infiltration capacity of PICP, thus it is expected that using sand as a friction agent during winter will decrease the infiltration capacity of PICP areas. This paper examines the effect of gritting of roads as winter maintenance on the infiltration capacity of PICP. Infiltration rates in the slits, the gaps between the pavers, with different fractions crushed sand applied as friction agent has been tested on laboratory column scale and in a small-scale pilot in a climate-controlled conditions. In the column test the saturated hydraulic conductivity decreased with 97 % when the fraction of crushed stone graded 0-2 % was increased from 0 % to 50%. In the following small-scale pilot, no similar decrease was observed.

Keyword: permeable interlocking concrete pavement, stormwater management, winter operation

1 Introduction

Both climate change and urbanization cause challenges for stormwater management. Urbanization leads to an increasing share of impervious surfaces, resulting in higher runoff volume and faster runoff peaks. This is accentuated by climate change driven change in rainfall patterns and more intense rainfall events (Hanssen-Bauer *et al.*, 2017; Willems *et al.*, 2012). At the same time are old common drainage pipes and systems not dimensioned for, and therefore not able to handle, the increase in flow. This resulting in increasing urban flooding (Miller and Hutchins, 2017).

There has been a change in stormwater management towards handling the increased stormwater locally instead of the traditional way of transporting it to recipients by pipes. Handling stormwater by draining developed areas in a more natural way by using the infiltration and storage capacity of semi-natural devices are collectively known as both Sustainable Urban Drainage Systems (SUDS) and Low Impact Development (LID) (WEF, 2012; Butler and Davies, 2011). Infiltration wales, raingardens, green roofs, permeable pavement and detention and retention reservoirs are all examples of SUDS (Butler and

Davies, 2011). An increasing number of municipalities in Norway are also restricting on the amount of runoff that can be led to the pipelines.

Norsk Vann, a national association representing Norway's water industry, has proposed a "three step strategy" for how stormwater should be handled. The first step is local infiltration of small rainfalls ($<20\text{ mm}$), the second step is to delay and detain medium rainfalls and the third step is to ensure safe flood paths for large rainfall events ($> 40\text{ mm}$)(Lindholm *et al.*, 2008). Permeable pavement is a SUDS that can contribute to the two first steps of the "three step strategy". If the infiltration capacity of the native soil is good, the permeable pavement will infiltrate the stormwater and contribute to maintaining the ground water level. If the ground gets saturated, or the infiltration capacity of the native soil is poor, water can be stored in the construction and still fulfill step two in the strategy. Necessary extra capacity can be achieved by connecting an extra tank to the underdrain and thereby increasing the detention capacity.

In cities and populated areas, hard surfaces are needed for both cars and people. Roads, parking spaces and walkways have to be made by hard surfaces, and often are open areas for people to enjoy made up of hard surfaces too. Normally these are paved with asphalt or other impermeable pavements, which contributes greatly to the runoff generation. Permeable pavement can, unlike most other SUDS, replace the impermeable surface. This gains the benefits of SUDS while maintain the hard surface needed for practical use. Permeable pavement is normally not recommended to use on heavily trafficked roads, but can be implemented on walkways, parking spaces and less trafficked areas (Eisenberg, Lindow and Smith, 2015). This allows for use on large areas, contributing heavily to reduction of the impermeable area of a city.

The use of permeable pavement has increased over the last years, and have particularly been implemented in USA, Australia and in European countries like the Netherlands and Germany. On the other hand, has the implementation of permeable pavement as a stormwater measure been slow in Norway. One reason for the low use of permeable pavement is the uncertainty connected to use in cold climate. The freezing temperature and winter maintenance of the roads could affect both the infiltration capacity and the structural integrity of the permeable pavement, and hence the effective lifespan of the permeable pavement, making decision makers uncertain. In Norway, and other countries with cold climate, is gritting sand, salt or a combination spread on roads as a part of the winter maintenance to reduce the risk of accidents occurring by increasing the friction (Nordheim and Thordarson, 2001). Even though normal procedure is to remove the applied sand, often by brushing, in the spring, it is inevitable that the sand has the possibility to affect the permeable pavement.

A laboratory study performed in Vermont, USA showed that the permeability of porous concrete decreased with 15 % by a single application of a sand and salt mixture at a rate of 0.12 g/cm^2 , but still remaining adequate to handle the anticipated rainfall events in Vermont (McCain and Dewoolkar, 2009). Henderson (2012) found that both the use of gritting sand and salt decreased the permeability of porous concrete located in Canada, but not to an unacceptable level. However, these studies have been performed on porous

concrete, as opposed to this study with permeable interlocking concrete. It is made of impermeable concrete pavers with permeable joints, so that the mentioned results will not necessarily apply to permeable interlocking concrete pavement.

A study on permeable interlocking concrete pavement performed by Lucke and Beecham (2011) found that even though the largest mass of sediments was accumulated in the aggregates, its large storage capacity caused it to not be a problem. They found that the sediments trapped in the joint material of the permeable interlocking concrete pavement were critical for the infiltration capacity of the pavement, which makes the effect of the gritting sand on the joint material likely to be crucial for the effect on the hydraulic function of the pavement.

There is a clear knowledge gap when it comes to how the application of sand as a part of the winter maintenance affects the infiltration capacity of permeable interlocking concrete pavement. Therefore, will this study further investigate how sand used for gritting during winter affects the infiltration rate of permeable interlocking concrete pavement through laboratory column test and a small-scale pilot test. The study will try to answer the following research questions:

1. Do the sediments of crushed sand influence the infiltration capacity of the gravel fillings in the slits?
2. To what extent represent the current practice of using sand during winter operations a problem to permeable interlocking concrete pavements?

2 Materials and method

2.1 Materials

Crushed gritting sand, joint material, material for the bedding and base layers, and concrete pavement was needed to perform the study. Due to experiments being performed during the fall it was not possible to obtain used gritting sand, only new gritting sand. Gritting sand used in Norway often have a grading of either 0-4 *mm* or 0-6 *mm* with a larger fraction of the larger particles (Rosten, 2012). Used gritting sand has been crushed by traffic after being applied to the road, and consequently having a larger fraction of the smaller particles. Knowing that the joint material used for permeable interlocking concrete paving normally have a grading of 2-5 *mm* to ensure sufficient infiltration capacity, the problem with clogging is connected mainly to material with grain size smaller than 2 *mm*. A study done by Balades et al. (1995) referred by Yong, McCarthy and Deletic (2013) also suggest that particle size influences clogging, since smaller particles will trap larger particles hence increasing the rate of clogging. Using new gritting sand in the experiments would therefore be expected lead to less clogging than using used gritting sand and would not be representative for the real situation. For this reason, gritting sand was substituted with crushed stone with particle size 0-2 *mm* for use in the experiments. The crushed stone was provided by Franzefoss section Vassfjell.

The joint material, the bedding layer and the concrete pavers were provided by the BIA-project Drensstein. The project includes a test site for permeable interlocking concrete pavement in Malvik, constructed during the fall and winter of 2019, and the same materials were used. The particle size was respectively 2-5 *mm*, 5-11 *mm* and 4-16 *mm* for the joint material, bedding layer and base layer.

2.2 Methods

In the present study, first a dry sieving test was performed to determine the grain size distribution of the crushed stone. Then a column test was performed to determine the saturated hydraulic conductivity of the joint material containing different fractions of crushed rock. Further a small pilot of a permeable interlocking concrete pavement was constructed to investigate if the results from the column test could be observed on a larger scale. Since the climatic component is interesting, the pilot experiment was performed in a climate lab with possibility to manipulate the temperature.

2.2.1 Grain size distribution

To determine the fraction of the different grain sizes in the crushed rock with grading 0-2 *mm* a grain size distribution curve was made. A dry sieving method was initially chosen, and the results were evaluated to see if a sedimentation test was needed. Chapter 5.1 in International Organization for Standardization (2016) says that if less than 10 % of the sample is smaller than 0.063 *mm* a sedimentation test is normally not required.

Three samples were taken of the crushed rock used in the study, to verify that the grain distribution curves obtained were representative. The weight of the three samples were 200.0 g, 200.0 g and 200.1 g. Since the maximum particle diameter should be 2 mm, the recommended minimum mass used in a test is 100 g (International Organization for Standardization, 2016). The samples were dried for 24 hours at 105 °C to ensure that there was no water left in the samples before performing the dry sieving.

Sieves with opening 4 mm, 2 mm, 1 mm, 500 μm, 250 μm, 63 μm and sealed bottom were used. A Retsch AS 200 machine was used for 50 minutes with an amplitude of approximately 75. It was sieved until one extra minute of sieving did not change the mass weight on any of the sieves by more than 1 % according to the requirements made by International Organization for Standardization (2016). International Organization for Standardization (2016) also requires that the masses on each sieve are compared to the maximum amount of soil that should be retained on each sieve.

Equation 1 shows how the fraction of soil passing each sieve was calculated (International Organization for Standardization, 2016):

$$f_n = \frac{m_1 + m_2 + \dots + m_n}{m} * 100 \% \quad (1)$$

Where f_n is the fraction passing the sieve (%), m_1 is the mass of soil passing the smallest mesh size (g), m_2 to m_n is the mass of soil passing the consecutive sieves up to the one considered (g) and m is the total dry mass of the sample (g).

2.2.2 Column tests

To test how the infiltration capacity of the joint material is affected by the presence of crushed rock the saturated hydraulic conductivity was tested. Plexiglas columns (450 mm long, 100 mm inner diameter and 5 mm wall thickness) constructed by Monrabal-Martinez, Ilyas and Muthanna (2017) were used. The columns were filled with 40 cm of joint material. All experiments were triplicated and the first column was filled up to 40 cm, the content weight and the two replicate columns were filled by weight. The test was repeated four times with increasing fraction of crushed rock mixed into the joint material. The five tests and the corresponding weight can be seen in Table 1.

Table 1: Shows the setup of the column tests with the weight percent of joint material and crushed rock and the total weight of the material for each test and the measuring time used for each test.

	Fraction joint material (Weight %)	Fraction crushed rock (Weight %)	Weight (kg)	Measuring time Δt (seconds)
Test 1	100	0	4.45	60
Test 2	75	25	4.50	60
Test 3	50	50	5.03	60
Test 4	25	75	5.10	300
Test 5	0	100	5.30	300

Using the column setup, a constant head test is performed where both the inlet water level and the outlet level is kept constant. The inlet water level is kept constant by a continuous supply of water in combination with an overflow outlet. The water used was regular tap water holding a temperature of $10\text{ }^{\circ}\text{C} \pm 0.5\text{ }^{\circ}\text{C}$ and the test was performed in room temperature of $20\text{ }^{\circ}\text{C}$.

Darcy's law was used according to International Organization for Standardization (2019) to obtain the saturated hydraulic conductivity:

$$K_{measured} = \frac{\Delta V \cdot L}{\Delta t \cdot A \cdot \Delta h} \quad (2)$$

Where ΔV is the volume of water (mL) collected at the outlet during a given measuring time Δt ($seconds$), A is the cross-sectional area (mm^2) of the columns, L (mm) is the length of the soil column and Δh is the pressure head difference (mm) between the head of water and the outlet as shown in Figure 1.

The outflow volume of water was measured by weight ($gram$) and converted to volume (mL) by a factor of 1000.30009 based on the tables for density given by Crittenden *et al.* (2012). All variables except for the measuring time were kept constant for all tests. The measuring time was initially set to 60 $seconds$, however for test 4 and 5 the measuring time was increased to 300 $seconds$ to be able to collect a reasonable amount of water and reduce the uncertainty. A picture of the setup can be seen in Figure 2.

International Organization for Standardization (2019) requires that the permeability should be consistent over four intervals of time, so the measuring continued until this was accomplished, and the permeability was averaged over these four samples.

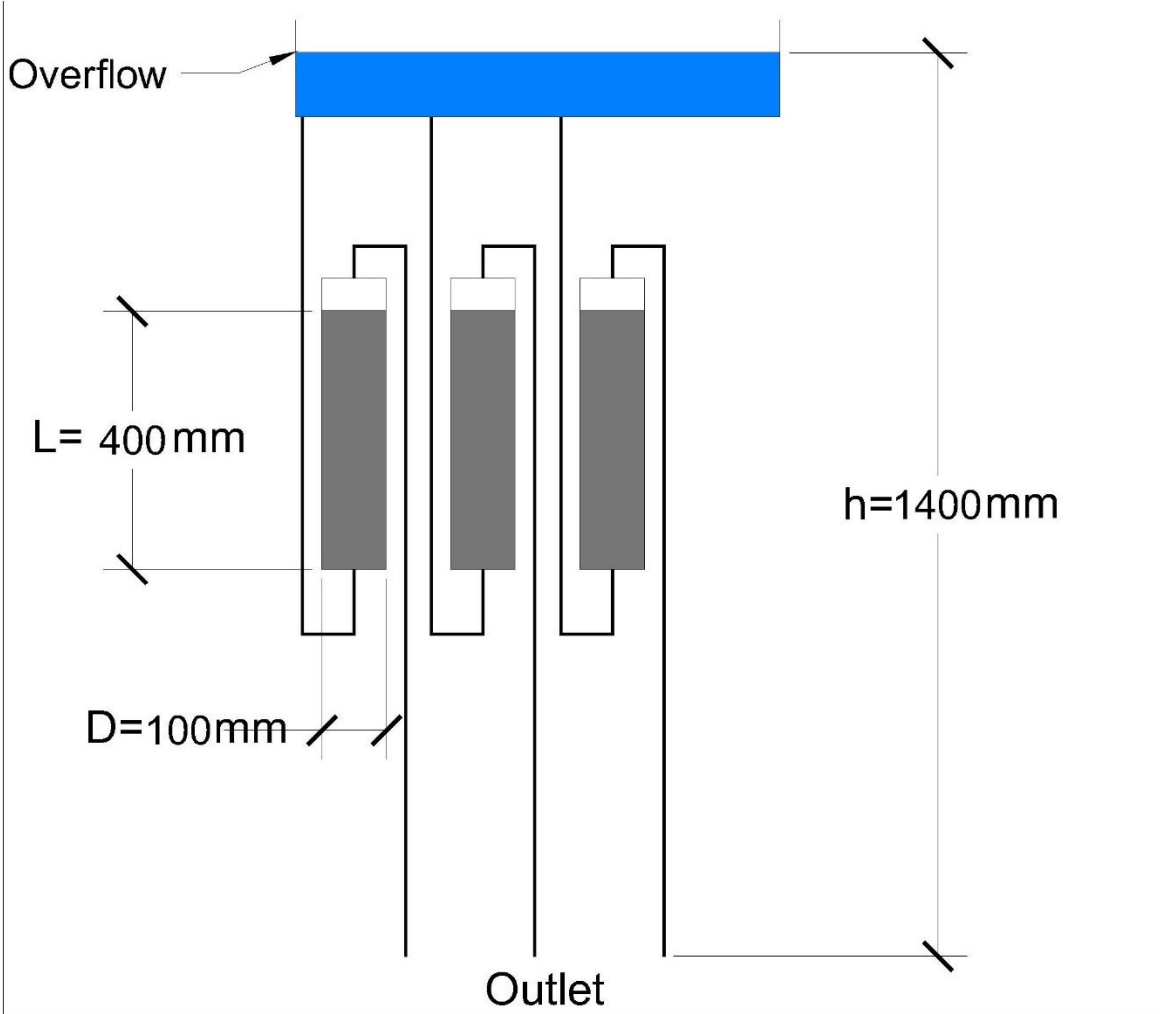


Figure 1: Illustration of the setup for the column test.

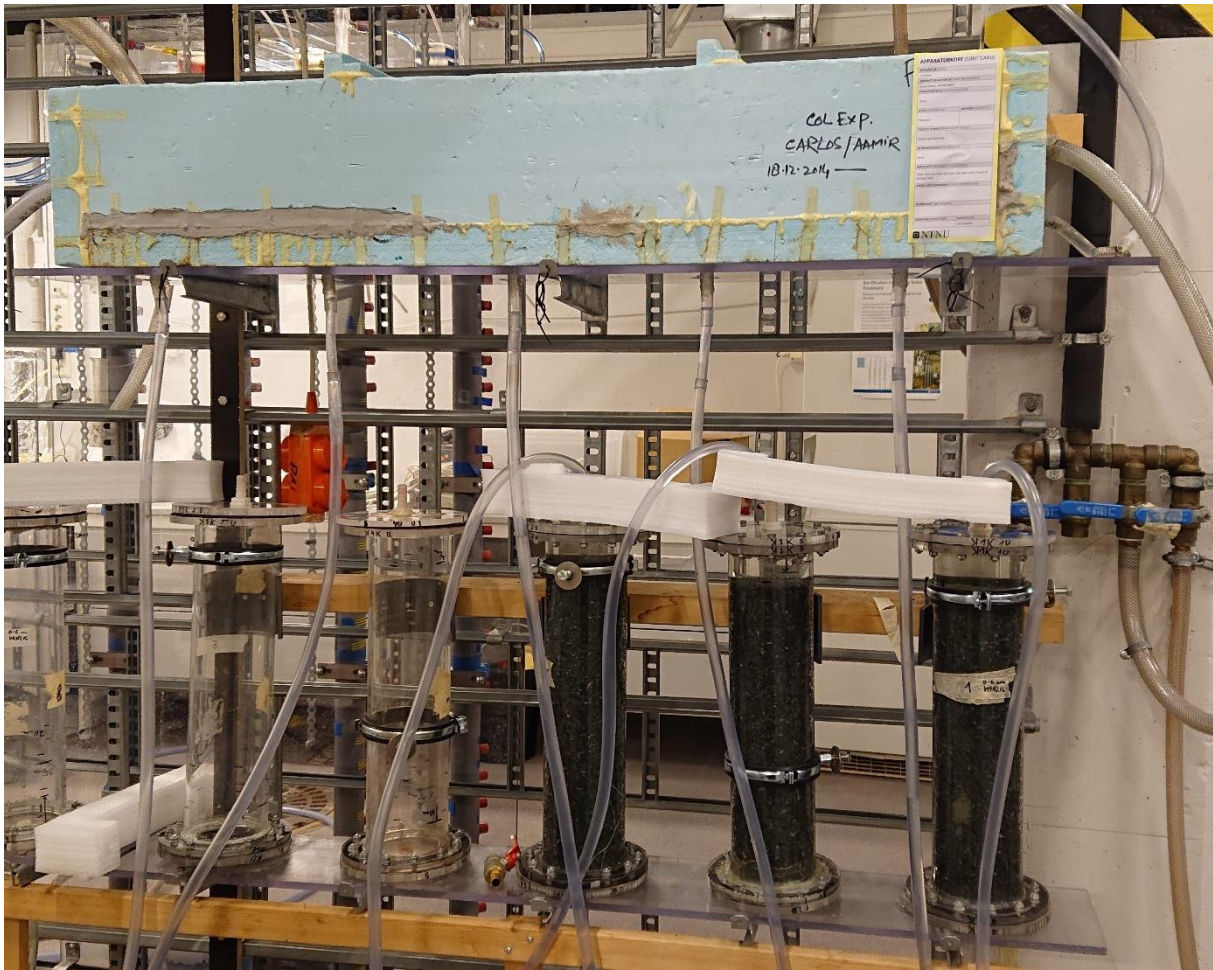


Figure 2: Picture of the setup for the column test. Photo: Heidi Jensen

Leakages from some of the columns lead to visible air bubbles in the water stream which affected the results, caused some of the columns to be rejected and the test repeated with a new, sealed column. The air bubbles also lead to a considerable fraction of the finer particles being washed out, which was observed visually and in the increase in effluent volume.

To compare the saturated hydraulic conductivities obtained, with a water temperature of 10 °C, to the results that was planned to be obtained in the pilot test the conductivity was adjusted to a temperature of 2 °C by using a factor of 0.78 based on the tables for dynamic viscosity of water (Crittenden *et al.*, 2012).

The tubes used to collect the water introduces a hydraulic head-dependent resistance and for highly permeable media this can lead to underestimation of the saturated hydraulic conductivity (Nijp *et al.*, 2017). The possible effect of the tubes was not evaluated in this study. Other possible uncertainties in the column test is that collection of water at the outlet over a given time was done manually, giving some error due to the human reaction time, and that the mixing of material could cause small differences between the columns.

2.2.3 Small scale pilot test

To test the results found in the column test the next step was to construct a pilot in the climate lab at SINTEF in Trondheim to evaluate if the results from the column test could be observed on a larger scale under freezing winter temperatures. To simulate winter conditions the pilot was frozen in the climate lab until the structure reached $-10\text{ }^{\circ}\text{C}$, before the temperature was turned up to room temperature and tap water cooled to $2 \pm 0.5\text{ }^{\circ}\text{C}$ applied. To reduce the time to reach a core temperature of $-10\text{ }^{\circ}\text{C}$, which based on Rafdal (2019) was estimated to take 7-10 days, the air temperature was set to $-15\text{ }^{\circ}\text{C}$ for the first three days, before it was increased to $-10\text{ }^{\circ}\text{C}$.

In the pilot a falling head test was performed to measure the hydraulic conductivity (International Organization for Standardization, 2019). This was done by manually applying 70 litres water, which would give an initial upstream water level of 10 cm if the entire amount of water could be applied before any infiltration occurred. The water was applied over approximately 60 seconds. The upstream and downstream water pressure was measured, and the pressure head difference and the outflow volume of water during a given time interval was calculated.

The pilot permeable interlocking concrete pavement was constructed inside a box constructed by Rafdal (2019). As illustrated in Figure 3, the permeable interlocking concrete pavement was constructed from bottom and up of 40 cm base layer, 5 cm bedding layer and 10 cm concrete pavers with permeable joint material. The waterproofness was ensured by coating the inside of the box with Icopal Blackline 1000, a 1.2 mm thick thermoplastic polyolefin membrane. The membrane could resist the pressure and possible sharp gravel edges. The weight of the bedding layer, pure joint material and joint material mixed with 50 percent crushed rock weighed respectively 54.84 kg, 9.60 kg and 9.00 kg. Between the pavement and the walls of the box there was a gap, which would not be there in a permeable interlocking concrete pavement constructed on site. To prevent water from being infiltrated here, it was filled with bubble wrap to ensure no horizontal flow into the gap, and tape was fastened with sealant to the pavement and wall to seal the surface to prevent vertical inflow to the gap. The joint area, which is the permeable area, covers approximately 6 % of the total area of the pavement, not included the four joints sealed by measuring instruments. The water was allowed to exit the box through a tap and collected in a box, with width 56 cm and length 77 cm.

To ensure adequate drainage to the outlet and prevent standing water in the box was the opposite corner from the tap elevated with an inclination of 1 % towards the outlet. To allow the water to distribute evenly and be infiltrated through the full area of the pavement the surface should be kept horizontal. This was by constructing all the layers of the pavement horizontally when the corner was elevated. By doing so the water head can be kept equal over the whole pavement.

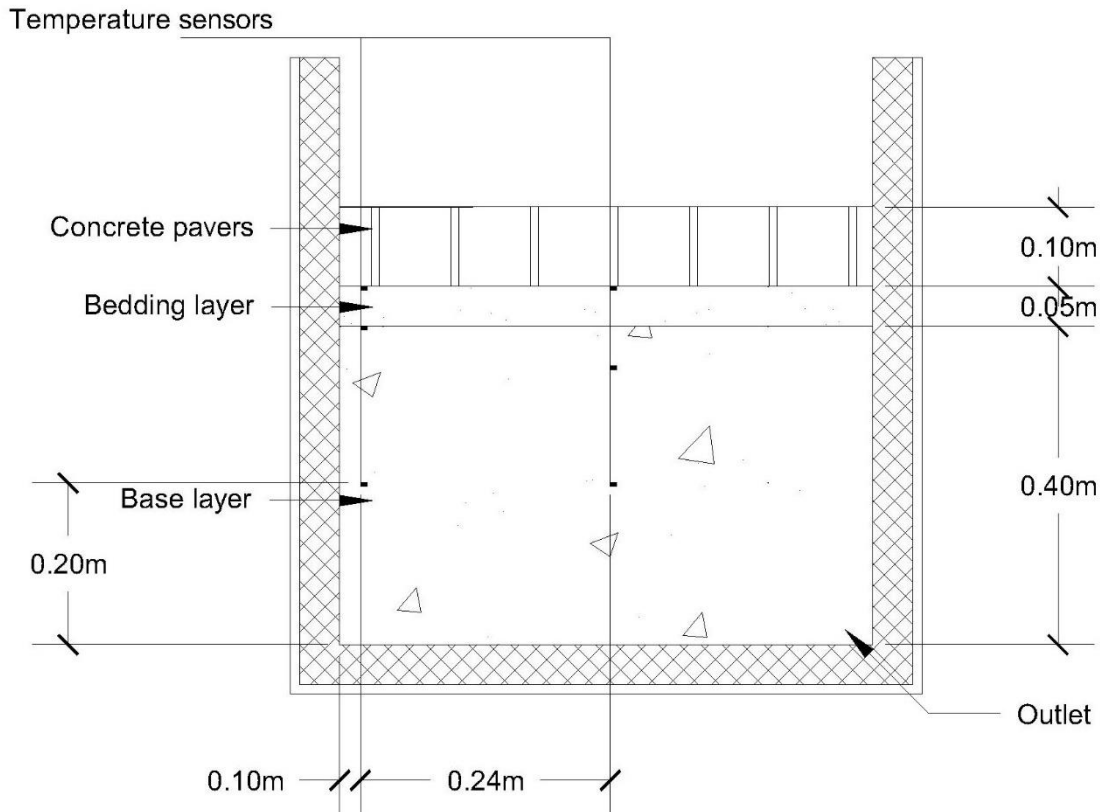


Figure 3: Construction of the permeable interlocking concrete pavement for the pilot with placement of the temperature sensors.

The pilot was instrumented, as seen in Table 2, to measure temperature and humidity inside the pavement construction, and pressure and temperature in the influent and effluent water. The pressure was measured by two VanEssen CTD-Divers installed above the permeable pavement in the box and by two Divers in the box where outflow water is collected. As the Divers measured the absolute pressure, including both the water pressure and the atmospheric pressure, a Baro-Diver measuring the atmospheric pressure was needed calculate the water level (vanEssen Instruments, 2016). Since the Diver first measure water pressure when the water level reach above the Diver-head, the box collecting the outflow water was prefilled with 2.5 cm of water.

There was also installed four humidity sensors measuring the humidity at different levels in the pavement. The pilot was equipped with six temperature sensors; two under the concrete pavers, two under the bedding layer and two in the base layer, 20 cm from the bottom. Three in the center of the box, 34 and 54 cm from the walls, and three towards the side, 10 and 54 cm from the walls, as seen in Figure 3. In addition, one temperature sensor was placed on top of the pavement and one in the box for effluent water to measure the water temperature. The placement of the instruments can be seen in Figure 3 and Figure 4.

Table 2: The instrumentation of the pilot

Parameter	Instrument	Number	Measuring interval	Comment
Soil moisture	Delta-T PR2 Profile Probe	4, measuring in 4 levels over the depth	30 s	
Soil temperature	Temperature probes	6, measuring at 2 places at 3 levels over the depth	30 s	
Water temperature	Temperature probes	1 in inlet and 1 in outlet	30 s	
Air temperature	Temperature probe	1	30 s	
Water level	VanEssen CTD-Diver	4, 2 over the pavement and 2 in the outlet	5 s	Plus, one Baro-Diver to enable transformation of absolute pressure to water level

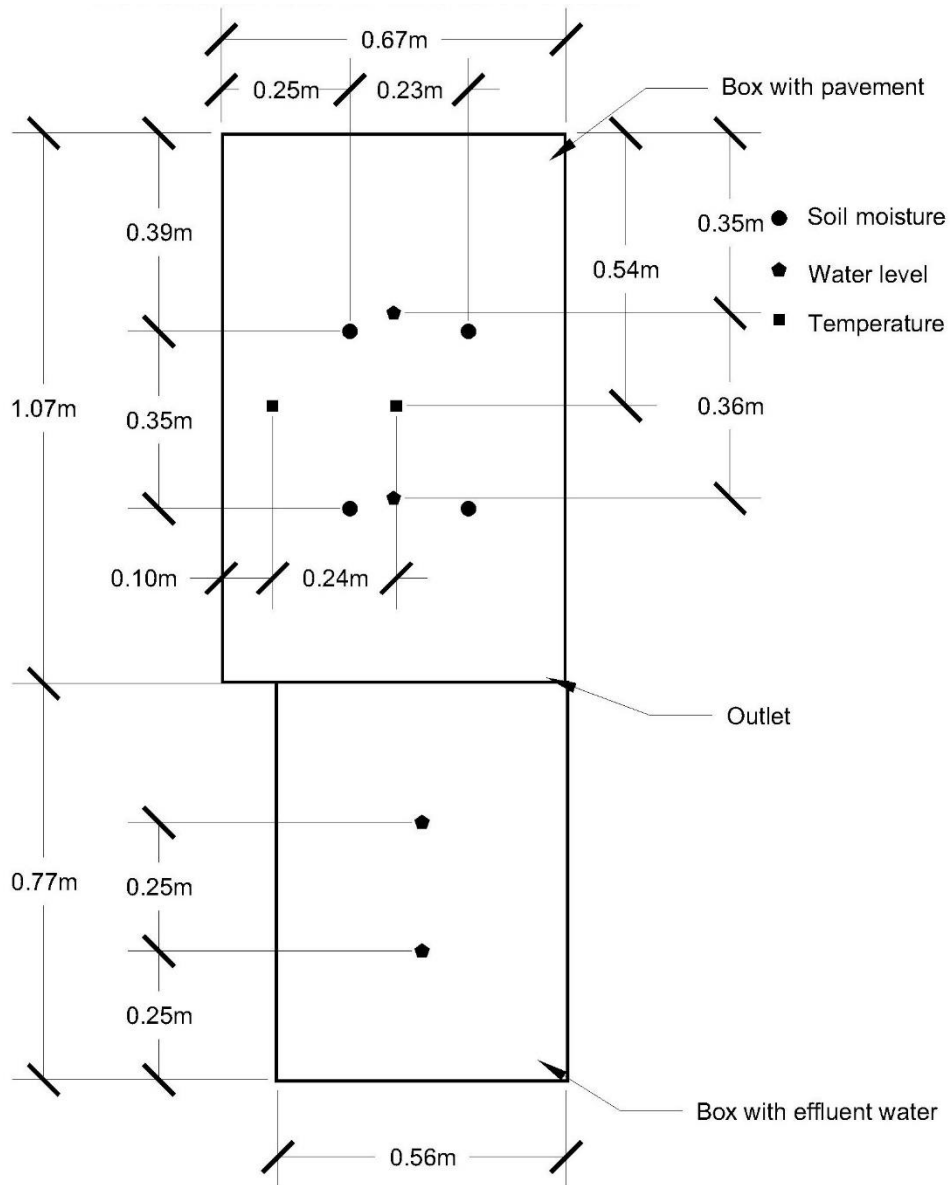


Figure 4: Figure showing the placement of the Divers, humidity and soil moisture sensors in the horizontal plan.

The water column (WC, cm) above the Diver was calculated by the following equation:

$$WC = 9806.65 \cdot \frac{P_{diver} - P_{baro}}{\rho \cdot g} \quad (3)$$

where P_{diver} is the pressure measured by the diver (cmH₂O), P_{baro} is the pressure measured by the barometer (cmH₂O), g is the acceleration due to gravity (9.81 m/s²) and ρ is the density of the water (1 000 kg/m³) (vanEssen Instruments, 2016).

Between the experiments the joint material was vacuumed and replaced. To enable vacuuming of the joints, a piece of a water hose with diameter of 2 cm was taped to the end of the vacuum cleaner hose. It was hard to ensure that all the joint material had

been removed from the narrow slits, which can explain the lower weight needed in the second experiment to fill the joints.

During the reference test with clean joint material the water was applied by pouring directly on the pavement, leading to some detaching of joint material when the water stream hit directly in the joint as shown in Figure 5. It also caused poor distribution of water, causing water to be infiltrated only through parts of the pavement. To avoid this, a wood board with 54 holes of size of 10 mm located in the middle of each concrete paver where constructed before the second test to enhance distribution of water. The size of the holes where chosen after testing to ensure that the water could be applied to the pavement during the same interval of time as in the first test. The setup of the pilot with the wooden board is shown in Figure 6 .



*Figure 5: Picture showing how the joint material have been lifted from the slits during the first test
Photo: Heidi Jensen*

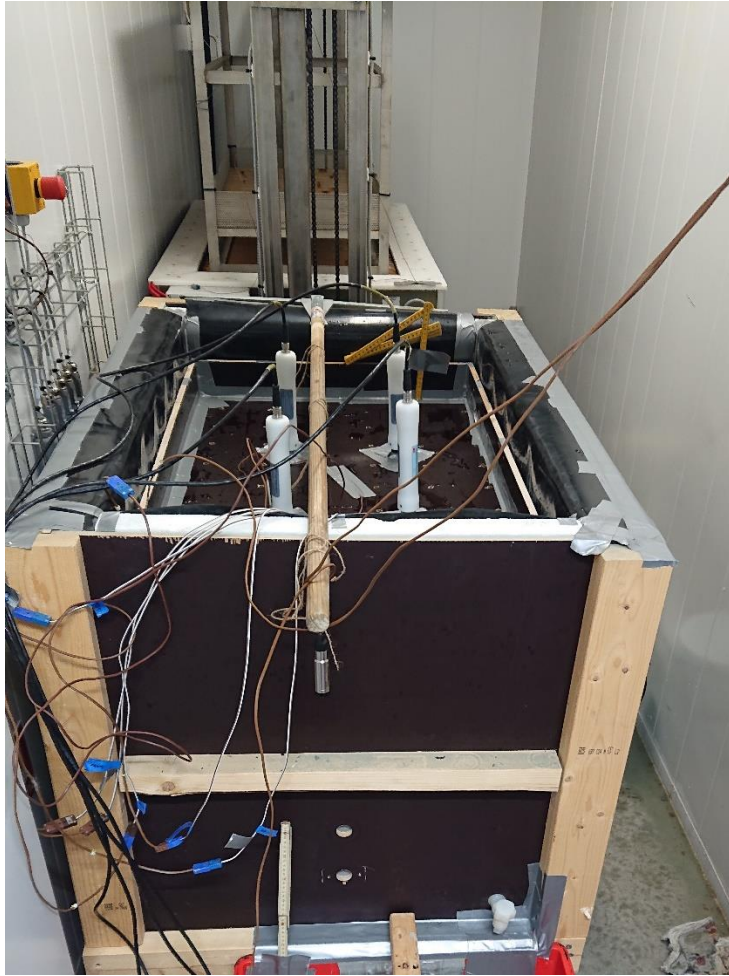


Figure 6: Picture showing the setup with the wooden board for test 2. Photo: Heidi Jensen

3 Results and Discussion

3.1 Grain size distribution

The results of the grain size sieving can be seen in Table 3 and Figure 7. Table 3 shows the weight of remaining material on each sieve and the fraction of the total mass passing the sieves, while Figure 7 shows the grain size distribution.

Table 3: Results from the sieving analysis with weight of remaining material on each sieve and the fraction of total mass passing the sieves.

	Test 1		Test 2		Test 3	
Sieve size (mm)	Weight material (g)	Fraction passing the sieve (%)	Weight material (g)	Fraction passing the sieve (%)	Weight material (g)	Fraction passing the sieve (%)
4	0.0	100.0	0.0	100.0	0.0	100.0
2	47.2	76.4	50.9	74.7	65.0	67.5
1	56.3	48.2	56.0	46.6	61.8	36.6
0.5	30.7	32.9	30.8	31.1	26.5	23.4
0.25	19.5	23.2	18.6	21.9	14.1	16.3
0.15	9.9	18.2	9.6	17.1	7.1	12.8
0.063	12.9	11.7	13.0	10.5	10.0	7.8
Bottom	23.6	0.0	21.1	0.0	15.6	0.0

Table 3 shows that the fraction of material smaller than 0.063 mm is larger than 10 % for both sample 1 and 2. Thus, a sedimentation test should have been performed. However, the fractions were barely over the limit, respectively 11.7 % and 10.5 %, and it was determined that a sieving analysis was adequate for the purpose of this study.

Figure 7 shows the grain size distribution for three samples from the crushed stone. It would be interesting to compare this grain size distribution curve with a grain size distribution curve of used gritting sand collected from roads in the spring. That can verify if the used material was similar to the crushed gritting sand.

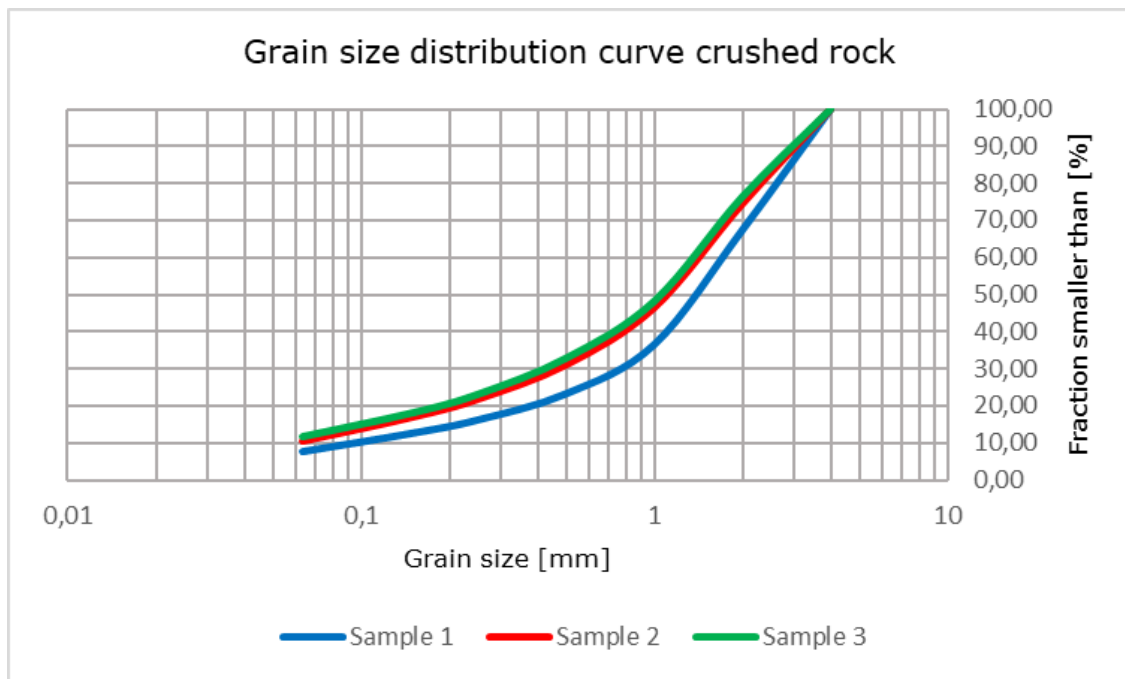


Figure 7: Grain size distribution for the crushed rock.

3.2 Column tests

The saturated hydraulic conductivity varied from an average of 2.97 mm/s in test 2 to an average of 0.05 mm/s in test 5. Figure 8 shows that the saturated hydraulic conductivity was almost unchanged when the fraction of crushed rock was increased to 25 %, it actually increased with 0.03 mm/s corresponding to 0.9 % increase. The largest observed drop in saturated hydraulic conductivity occurs when the fraction of crushed rock was increased from 25 % to 50 %. Then the saturated hydraulic conductivity measured was 0.21 mm/s , which was a reduction of 93 % compared with the measured saturated hydraulic conductivity of pure joint material.

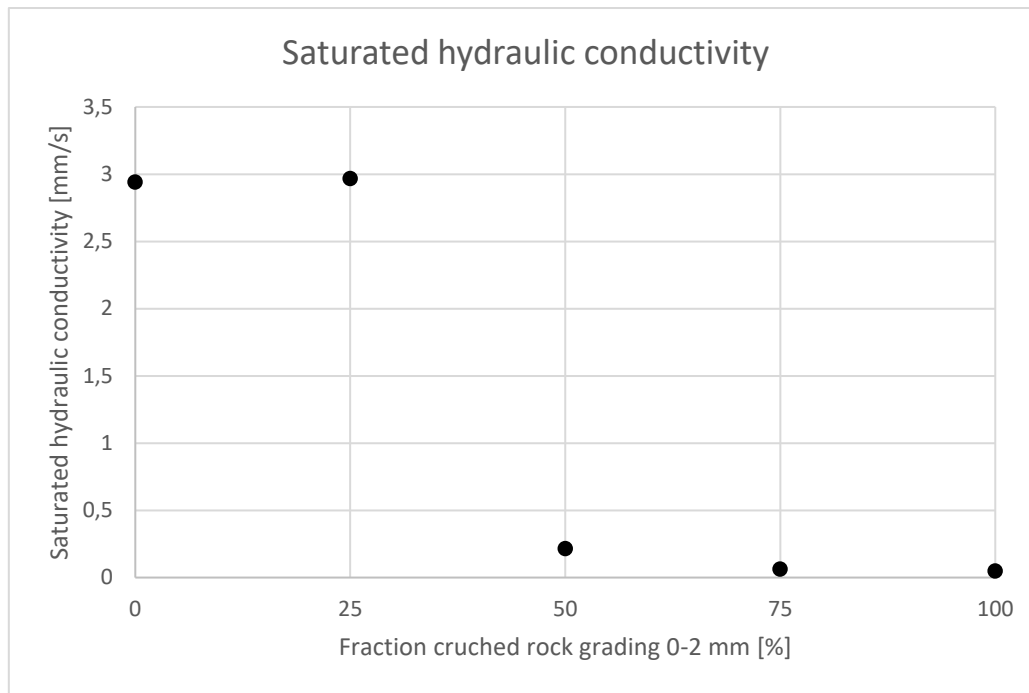


Figure 8: The plot shows how the saturated hydraulic conductivity varies with the fraction of crushed stone in the joint material.

For both test 3 and 4 the results from one column were clearly deviating from the average of the other two columns, being respectively 271 % and 150 % of the average. Consequently, the column was omitted when the average was calculated. The deviation could be caused by a leakage that was not visually detected or that the material used in those columns deviated from that used in the other columns. The joint material and crushed rock were mixed manually for each test, which may have resulted in imperfect mixing.

Borgwardt (2006) found a positive correlation between the percentage of joint area and the infiltration rate of new permeable interlocking concrete. Further saying that the infiltration rate of a newly made permeable interlocking concrete pavement is dependent on the permeability of the joint material, joint ratio and how the pavement is constructed. This means that the saturated hydraulic conductivity measured in the column test is not the only parameter affecting the saturated hydraulic conductivity a permeable interlocking concrete pavement constructed with the tested joint filling material will have.

Pezzaniti, Beecham and Kandasamy (2009) found a reduction in hydraulic conductivity of 59–75 % when a simulation of 35 years of sediment loading was performed in the laboratory. Following a parking lot constructed with permeable pavers Kumar *et al.* (2016) measured a reduction in infiltration rate of 85 %. Following the same pavement, the joint ratio was unchanged, and the reduction is mainly caused by the clogging of the joint material. Compared to that, the introduction of 50 % crushed rock in this study reduced the saturated hydraulic conductivity with 93 %.

3.3 Pilot test

The pilot test was performed by first freezing the pilot down to $-10\text{ }^{\circ}\text{C}$ before turning the temperature up and applying water to perform a falling head test as described in 2.2.3. The temperature graphs for the two tests can be seen in Figure 13 to Figure 16 in Appendix B.

In Figure 9 the effluent flow calculated based on the water level be seen. The flow values are calculated by dividing the increase in water volume over 60 seconds by 60 seconds to obtain the average flow (L/s) each minute. Since the water level was measured every 5th second the calculations were first made to obtain the average flow for 5 seconds at the time, but then the flow fluctuated around zero. This could be because the increase in water level in 5 seconds is too small to get consistent readings. As seen in Figure 9 even with time step of 60 seconds particularly the calculated outflow for test 2 varies a lot from minute to minute, which can indicate that the change in water level was too small for the Divers to get accurate enough readings. However the graph indicates that maximum outflow rate was slightly higher for the permeable pavement with 50 % crushed rock than for the test with clean joint material.

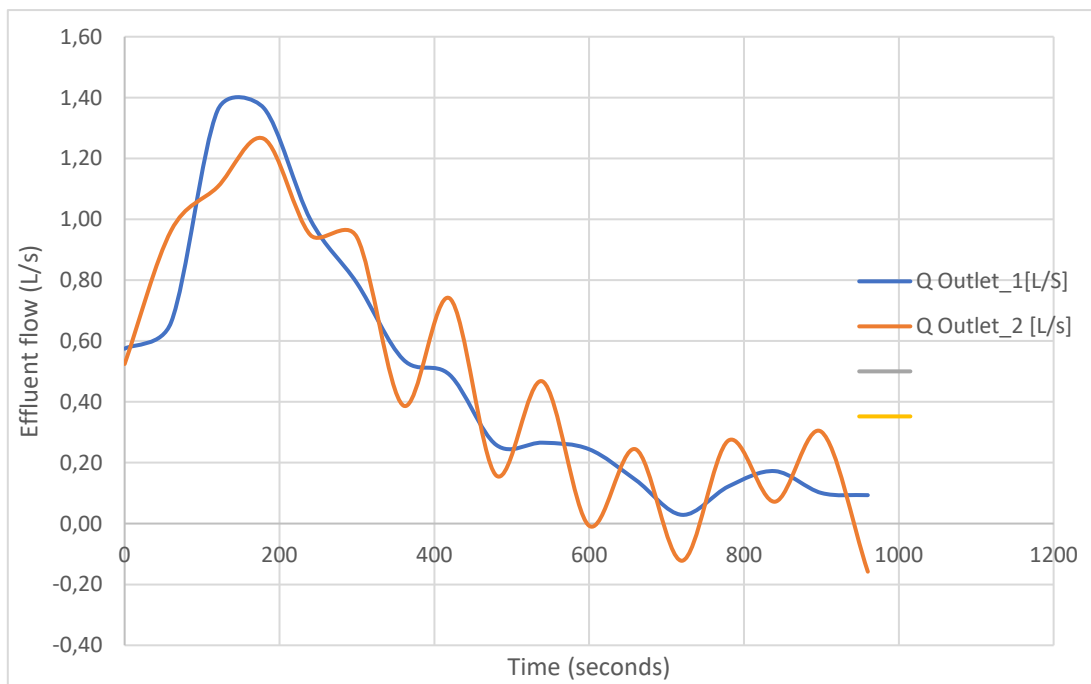


Figure 9: Graph showing the effluent flow based on the water level measured by the to Divers in the effluent box for both experiments.

By visual observation there was observed no ponding on the pavement in test 1 and minimal ponding in test 2. In test 1 the water was infiltrated faster than it was possible to apply the water. Between test 1 and test 2 a wooden board with holes to was added to the setup in order to apply the water directly onto the concrete pavers to allow for water to spread over the whole area and avoid joint material from detaching. As a consequence, it was harder to examine the ponding visually and a small ponding formation cannot be excluded. In addition, the water was distributed over the whole

pavement and infiltrated, while it in test 1 was poured directly on one small area of the pavement and infiltrated before it reached to flow out over a larger area of the pavement. This could allow for the same amount of water being infiltrated during the same amount of time even with a lower hydraulic conductivity.

In the effluent there was visually observed that there was washed out fine particles during both tests. During the first test these fine particles was expected to have been washed out from the base layer, since fine particles were observed in this layer during construction. However, the amount of fine particles in the effluent during the first test were reduced to a degree that the effluent water was approximately clear. Therefore, it is believed that most of the effluent fine particles observed during the second test originated from the crushed rock in the joint material. The fact that the fine particles could be washed out, in comparison to when the saturated hydraulic conductivity was measured in the column test, could affect the effect from the crushed rock on the hydraulic conductivity.

Based on the results from the soil moisture sensors, seen in Figure 10 to Figure 14 in appendix B, introduction of the wooden board to spread the inflow water over the whole pavement had some effect. Showing that both sensor 3 and sensor 4 measured increased peak soil moisture at the upper measuring level (40 cm from the bottom) during the second test, the water was clearly infiltrated over larger part of the pavement. Sensor 2 shows no change either over time or between tests and is therefore assumed to give incorrect measurements and not taken into consideration. For further tests performed in the pilot the wooden board should be used to ensure infiltration over the whole area.

To properly evaluate the effect different parameters have on the hydraulic performance of the permeable interlocking concrete pavement only one parameter should be varied at det time. In this study both the scale and the temperature were changed between the column test and the pilot test. However, in this study the main varied parameter was the fraction of crushed rock in the joint material, and its effect which was evaluated when test 1 and test 2 were compared. Due to limited time, and the long time needed to execute each experiment and some initial problems acquiring the necessary materials, there was only time to carry out two experiments. For further experiments an improved method of applying water at a higher rate need to be found. To reduce variations in the calculated outflow, the water collection box should have a smaller area. Then the changes in the water level will increase at the same outflow rate, reducing effect of the uncertainties in the measurements from the Divers.

In field studies performed on permeable interlocking concrete it is found that most of the clogging occurs in the top centimeters of the joints (Borgwardt, 2006; Balades *et al.*, 1995). When in this experiment the 50 % crushed rock is evenly distributed through the depth of the joint. This can lead to underestimation the amount of gritting sand needed for any possible effect to occur. Since the weight of crushed rock needed to get a fraction of 50 % gritting sand in the whole joint material is larger than needed to accumulate the same percent only in the top centimeters.

4 Conclusion

In the column test there was observed a reduction in the measured saturated hydraulic conductivity of the joint material with 93 % when the fraction of crushed rock increased from 25 % to 50 %, showing that the sediments of crushed rock will influence the infiltration capacity of the joint material. To verify the effect of crushed gritting sand grain s size distribution curve is necessary to compare with the one for crushed rock grading 0-2 *mm*.

During the pilot test of the permeable interlocking concrete the infiltration rate were too high to allow for measurements of the falling head to perform, making it impossible to calculate the hydraulic conductivity. As a result of this it was not possible to compare the hydraulic conductivity from the pilot with clean joint material and with 50 % crushed rock to see if the reduction found in the column test could be observed on a larger scale. On the other hand, comparing the effluent flow rate from the two test it could seem that if one had slightly better conductivity it would be the joint material with 50 % crushed rock. As a result of this the study gives no reason to believe that the current practice of sanding during winter has represents a problem for the use of permeable interlocking concrete pavements.

Between the two pilot tests there was introduced an improvement to the method to improve the distribution of the applied water. However, the method still needs further development including a more suitable way of applying water, to enable the use of a falling head test calculation of the hydraulic conductivity, or a decision to measure the hydraulic conductivity using a different method.

5 Further work

After results have been obtained from the pilot, doing measurements on permeable interlocking concrete pavement in field should be the next step. When doing studies in field the use of gritting sand will not be the only parameter affecting the changes in infiltration rate, so it would be an idea to have to equal areas with permeable interlocking concrete next to each other where the only difference is the use of sand during winter.

To answer research question 2: "To what extent represent the current practice of using sand during winter operations a problem to permeable interlocking concrete pavements?" there is also needed information about the extent of gritting during winter. This information will have large variations, both from type of road, municipality, climatic conditions, and from winter to winter. So, it is either needed to look at specific places and collect information about the use of gritting sand there or look at the variation of gritting sand applied on areas where permeable interlocking concrete pavement is an option to use. In addition, there is needed an estimation on how much of the applied gritting sand accumulates in the permeable pavement, since only this fraction of the gritting sand can represent a problem to the permeable pavement. The fraction that ends up on the side of the paved area or is removed by brushing in the autumn does not. It might be possible to collaborate with the municipality to find this.

References

- Balades, J. *et al.* (1995) Permeable pavements: pollution management tools, *Water Science & Technology*, 32(1), pp. 49-56.
- Borgwardt, S. (2006) Long-term in-situ infiltration performance of permeable concrete block pavement, *8th International Conference on Concrete Block Paving, San Francisco, California USA*.
- Butler, D. and Davies, J. W. (2011) *Urban Drainage*. 3rd edn. Abingdon, Oxon: CRC Press.
- Crittenden, J. C. *et al.* (2012) *MWH's Water Treatment: Principles and Design*. 3rd edn. New Jersey: John Wiley & Sons.
- Eisenberg, B., Lindow, K. C. and Smith, D. R. (2015) *Permeable Pavements*. Reston: American Society of Civil Engineers.
- Hanssen-Bauer, I. *et al.* (2017) *Climate in Norway 2100 - a knowledge base for adaptation*. (NCCS report 1/2017). Oslo: NCCS. Available at: <https://www.miljodirektoratet.no/globalassets/publikasjoner/M741/M741.pdf> (Accessed: 15.10.2019).
- Henderson, V. (2012) *Evaluation of the Performance of Pervious Concrete Pavement in the Canadian Climate* Doctor thesis, University of Waterloo.
- International Organization for Standardization (2016) ISO 17892-4:2016 Geotechnical investigation and testing - Laboratory testing of soil. Part 4: Determination of particle size distribution. Geneva: International Organization for Standardization.
- International Organization for Standardization (2019) ISO 17892-11:2019 Geotechnical investigation and testing - Laboratory testing of soil - Part 11: Permeability tests. Geneva: International Organization for Standardization.
- Kumar, K. *et al.* (2016) In-situ infiltration performance of different permeable pavements in an employee used parking lot – A four-year study, *Journal of Environmental Management*, 167, pp. 8-14. doi: 10.1016/j.jenvman.2015.11.019.
- Lindholm, O. *et al.* (2008) *Veiledning i klimatilpasset overvannshåndtering (Guide in climate adapted handling of stormwater)*. (Norsk Vann report 162- 2008). Hamar: Norsk Vann. Available at: <https://www.norsk vann.no/> (Accessed: 6.09.2019).
- Lucke, T. and Beecham, S. (2011) Field investigation of clogging in a permeable pavement system, *Building Research & Information*, 39(6), pp. 603-615. doi: 10.1080/09613218.2011.602182.
- McCain, G. N. and Dewoolkar, M. M. (2009) Strength and Permeability Characteristics of Porous Concrete Pavements, *Transportation Research Board Annual Meetings, Washington, DC*.
- Miller, J. D. and Hutchins, M. (2017) The impacts of urbanisation and climate change on urban flooding and urban water quality: A review of the evidence concerning the

- United Kingdom, *Journal of Hydrology: Regional Studies*, 12(C), pp. 345-362. doi: 10.1016/j.ejrh.2017.06.006.
- Monrabal-Martinez, C., Ilyas, A. and Muthanna, T. (2017) Pilot Scale Testing of Adsorbent Amended Filters under High Hydraulic Loads for Highway Runoff in Cold Climates, *Water*, 9(3), pp. 230. doi: 10.3390/w9030230.
- Nijp, J. J. *et al.* (2017) A modification of the constant-head permeameter to measure saturated hydraulic conductivity of highly permeable media, *MethodsX*, 4(C), pp. 134-142. doi: 10.1016/j.mex.2017.02.002.
- Nordheim, H. and Thordarson, S. (2001) *Winter maintenance practice in the northern periphery. Rodex 1-sub-project B State-of-the-art study report*. Public Road Administration of Scotland. Available at: <http://www.roadex.org> (Accessed: 30.09.2019).
- Pezzaniti, D., Beecham, S. and Kandasamy, J. (2009) Influence of clogging on the effective life of permeable pavements, *Proceedings of the ICE - Water Management*, 162(3), pp. 211-220. doi: 10.1680/wama.2009.00034.
- Rafdal, A. (2019) *Innvirkning av frost på grunne overvannsystemer (Impact of frost on shallow overwater systems)*. Master Thesis, Norwegian University of Science and Technology. Available at: <http://hdl.handle.net/11250/2621015> (Accessed: 01.10.2019).
- Rosten, O. M. (2012) *Litteraturstudie Fastsandmetoden (Literature review on the frozen sand method)*. Oslo: Statens Vegvesen. Available at: https://www.vegvesen.no/attachment/644949/binary/967660?fast_title=10+Litteraturstudie+fastsand.pdf (Accessed: 30.09.2019).
- vanEssen Instruments (2016) *Product manual: Diver*. Available at: <http://www.vanessen.com/manuals> (Accessed: 26.10.2019).
- WEF (2012) *Design of urban stormwater controls*. 2nd edn. New York: WEF Press.
- Willems, P. *et al.* (2012) Climate change impact assessment on urban rainfall extremes and urban drainage: Methods and shortcomings, *Atmospheric Research*, 103, pp. 106-118. doi: 10.1016/j.atmosres.2011.04.003.
- Yong, C. F., McCarthy, D. T. and Deletic, A. (2013) Predicting physical clogging of porous and permeable pavements, *Journal of Hydrology*, 481, pp. 48-55. doi: 10.1016/j.jhydrol.2012.12.009.

Appendices

A. Column test

The effluent water volume measured in the five column test can be seen bellow in Table 4 to Table 8.

Test 1: 100 percent joint material and 0 percent crushed rock.

Table 4: Effluent water volume for test 1.

	Column 1	Column 2	Column 3
Sample 1	4999.3 g	4862.0 g	4862.6 g
Sample 2	4976.1 g	4836.1 g	4734.4 g
Sample 3	4905.2 g	4829.9 g	4684.0 g
Sample 4	4969.1 g	4791.7 g	4723.4 g
Average	4962.4 g	4829.9 g	4751.1 g

Test 2: 75 percent joint material and 25 percent crushed rock.

Table 5: Effluent water volume for test 2.

	Column 1	Column 2	Column 3
Sample 1	5032.3 g	5654.7 g	4163.5 g
Sample 2	5027.1 g	5504.3 g	4057.2 g
Sample 3	4997.7 g	5589.7 g	4098.2 g
Sample 4	4922.6 g	5593.1 g	4077.3 g
Average	4994.9 g	5585.5 g	4099.1 g

Test 3: 50 percent joint material and 50 percent crushed rock.

Table 6: Effluent water volume for test 3.

	Column 1	Column 2	Column 3
Sample 1	326.8 g	1261.6 g	375.0 g
Sample 2	342.9 g	1297.9 g	367.6 g
Sample 3	330.7 g	1249.0 g	377.4 g
Sample 4	305.3 g	1322.7 g	396.4 g
Average	326.4 g	1282.8 g	379.1 g

Test 4: 25 percent joint material and 75 percent crushed rock.

Table 7: Effluent water volume for test 4.

	Column 1	Column 2	Column 3
Sample 1	1200.8 g	500.8 g	593.8 g
Sample 2	1221.1 g	458.7 g	543.8 g
Sample 3	1261.2 g	451.3 g	531.5 g
Sample 4	1243.4 g	461.2 g	537.5 g
Average	1231.6 g	468.0 g	551.7 g

Test 5: 0 percent joint material and 100 percent crushed rock.

Table 8: Effluent water volume for test 5.

	Column 1	Column 2	Column 3
Sample 1	435.4 g	312.3 g	443.9 g
Sample 2	409.2 g	400.1 g	372.7 g
Sample 3	446.6 g	348.5 g	348.6 g
Sample 4	432.9 g	305.3 g	398.9 g
Average	431.0 g	341.6 g	391.0 g

Using the variables in Table 9 and the average effluent water volume for each column

from Table 4 to Table 8 in Darcy's equation the average saturated hydraulic conductivity for each column is found and can be seen in Table 10.

Table 9: Variables used in Darcy's formula to calculate the saturated hydraulic conductivity.

L [mm]	Δh [mm]	Δt test 1, 2 and 3 [seconds]	Δt test 4 and 5 [seconds]	A [mm²]
400	1400	60	300	$\pi \cdot 50^2$

Table 10: Saturated hydraulic conductivity for all three columns for each test and the average value for the tests.

	Test 1	Test 2	Test 3	Test 4	Test 5
Column 1	3.01 mm/s	3.03 mm/s	0.20 mm/s	0.15 mm/s	0.05 mm/s
Column 2	2.93 mm/s	3.39 mm/s	0.78 mm/s	0.06 mm/s	0.04 mm/s
Column 3	2.88 mm/s	2.49 mm/s	0.23 mm/s	0.07 mm/s	0.05 mm/s
Average	2.94 mm/s	2.97 mm/s	0.21 ^a mm/s	0.06 ^b mm/s	0.05 mm/s

a) Only column 1 and 3 have been used when calculating the average

b) Only column 2 and 3 have been used when calculating the average.

In both test 3 and test 4 there is one column which deviate clearly from the average calculated without including that result, with respectively 271 percent and 150 percent. There were no leakages, air bubbles or washout of fines visually observed during the tests, so the reason by the high saturated hydraulic conductivity is not clear even though this can be the reason despite it not being visually observed. Another possible explanation can be that the material used to fill those columns had a slightly different composition than the other despite the effort made to mix the joint material and crushed rock completely. As a consequence, column 2 in test 3 and column 1 in test 4 have not been used when calculating the average saturated hydraulic conductivity for the tests.

B. Pilot test

The measurements from humidity sensor during pilot test 1 are shown in Figure 10 to Figure 13, and for pilot test 2 in Figure 14 to Figure 17. The soil temperature during the freezing period and after the air temperature was turned up are shown in Figure 18 and Figure 19, and Figure 20 and Figure 21, for respectively pilot test 1 and pilot test 2.

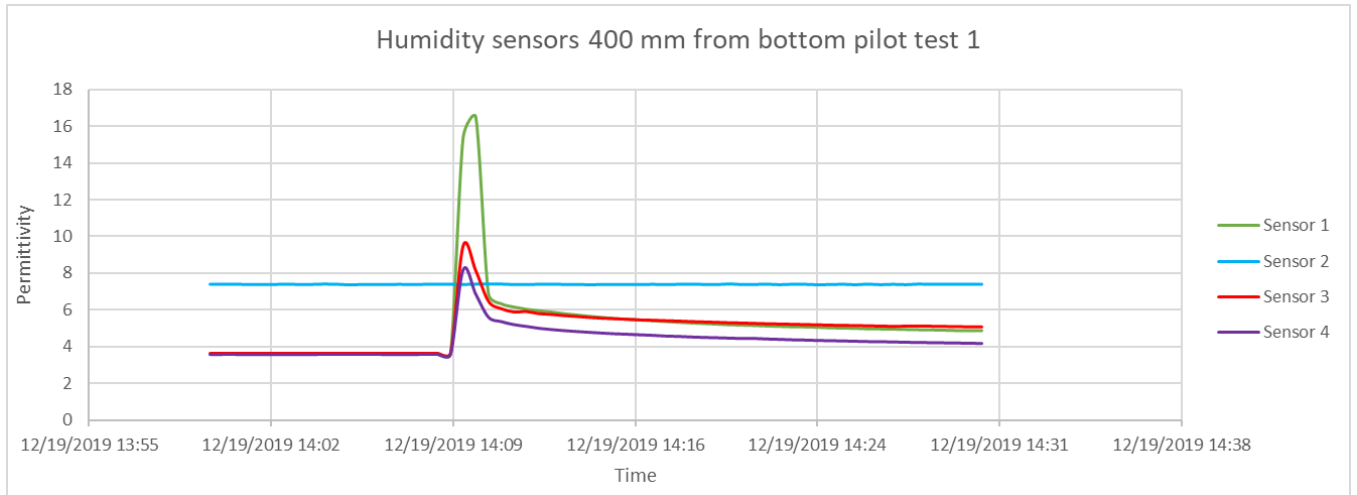


Figure 10: Graph showing the measurements from the humidity sensor 40 cm from the bottom during pilot test 1.

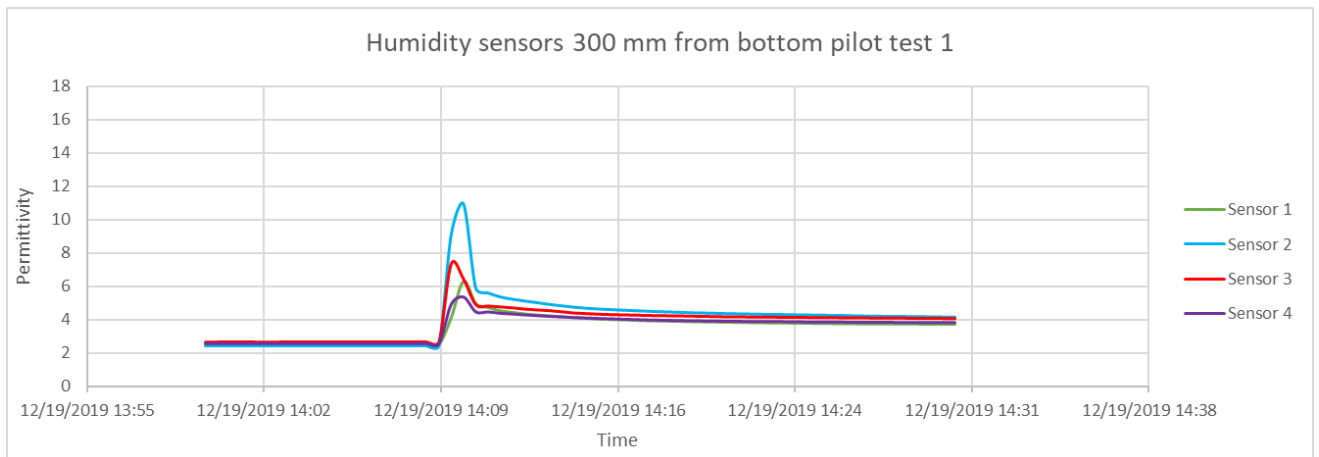


Figure 11: Graph showing the measurements from the humidity sensor 30 cm from the bottom during pilot test 1.

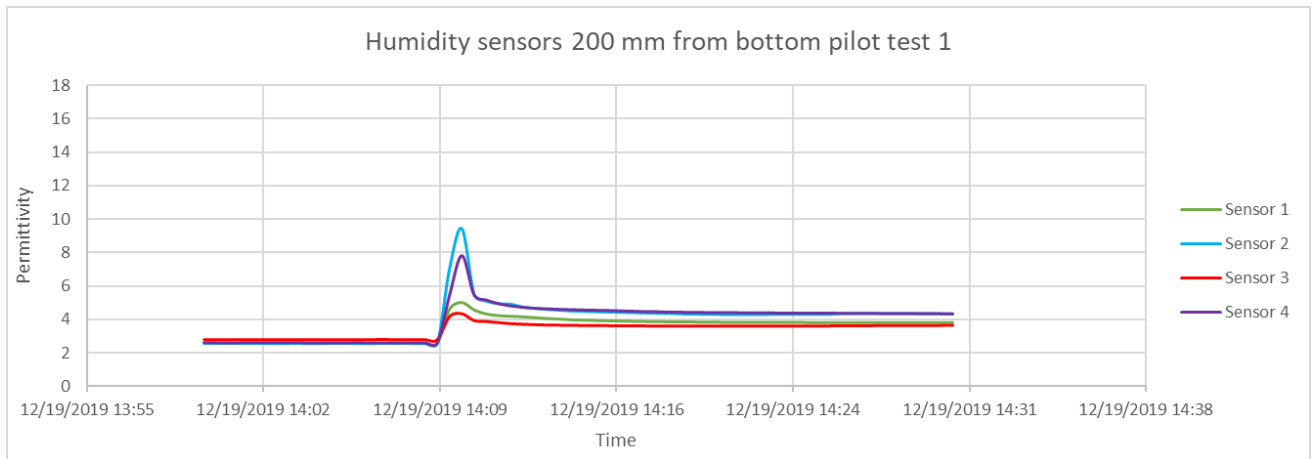


Figure 12: Graph showing the measurements from the humidity sensor 20 cm from the bottom during pilot test 1.

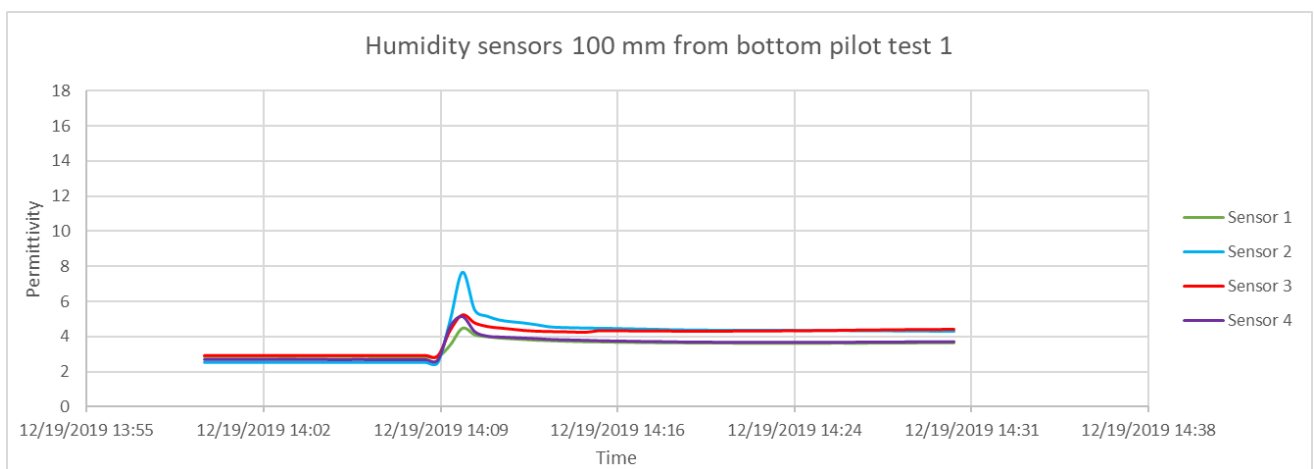


Figure 13: Graph showing the measurements from the humidity sensor 10 cm from the bottom during pilot test 1.

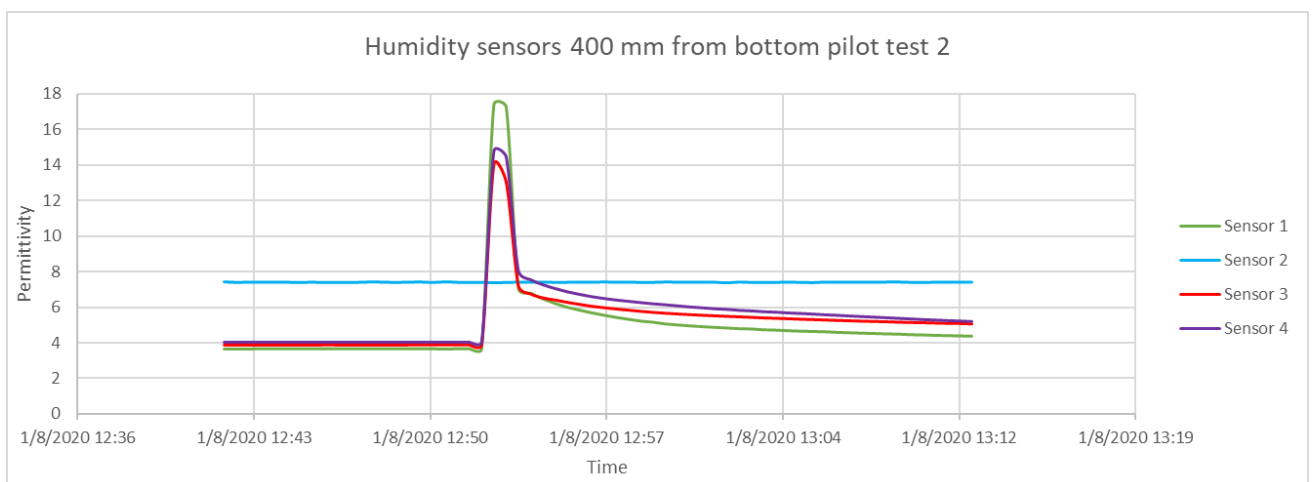


Figure 14: Graph showing the measurements from the humidity sensor 40 cm from the bottom during pilot test 2.

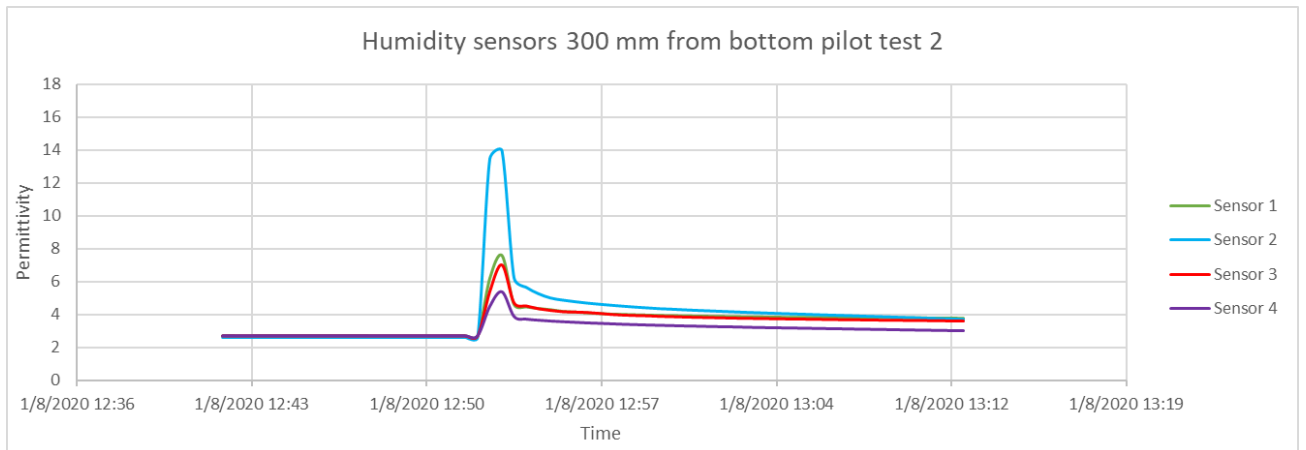


Figure 15: Graph showing the measurements from the humidity sensor 30 cm from the bottom during pilot test 2.

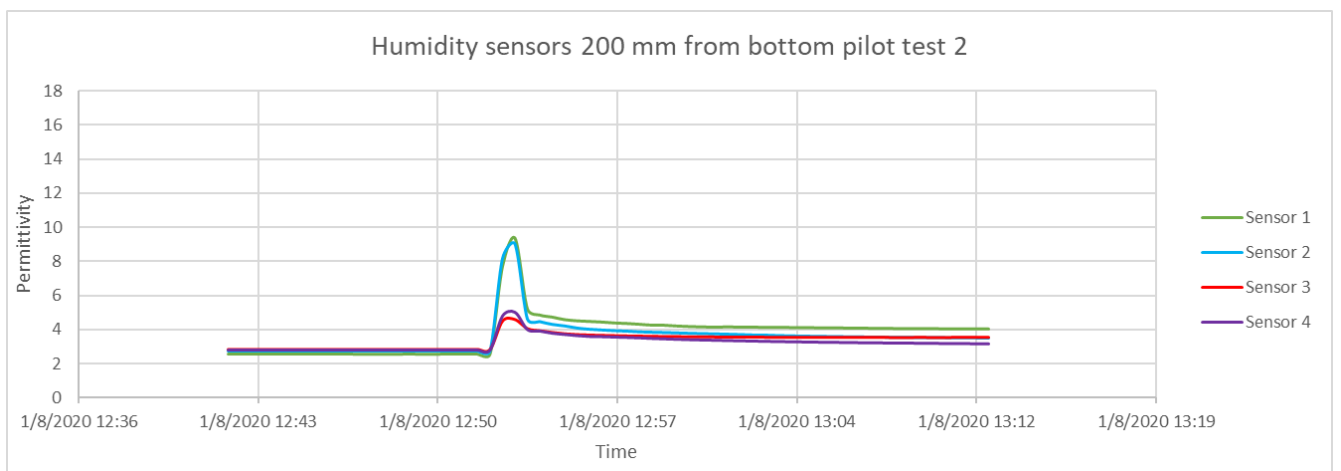


Figure 16: Graph showing the measurements from the humidity sensor 20 cm from the bottom during pilot test 2.

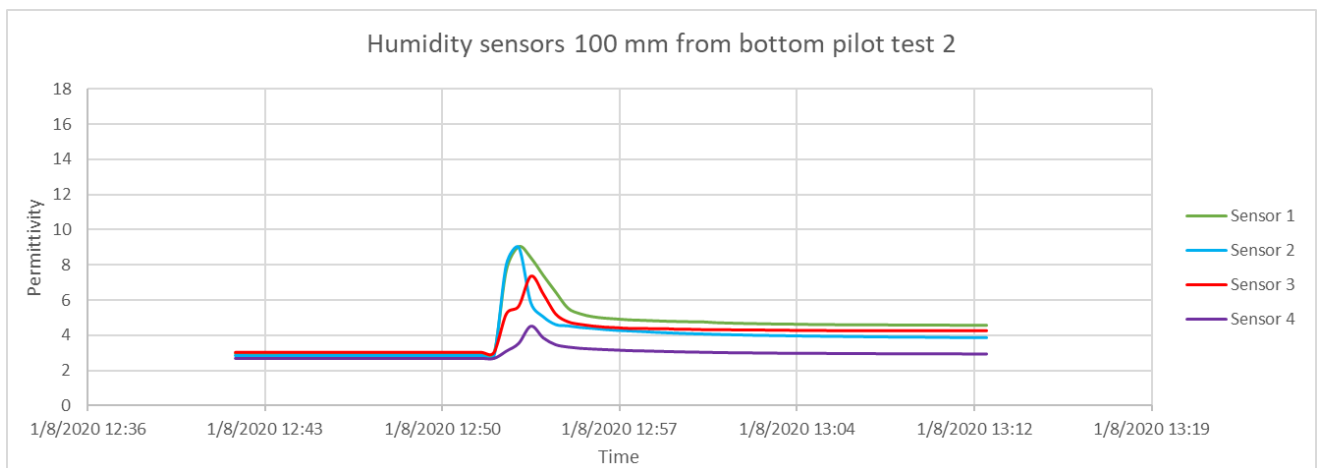


Figure 17: Graph showing the measurements from the humidity sensor 10 cm from the bottom during pilot test 2.

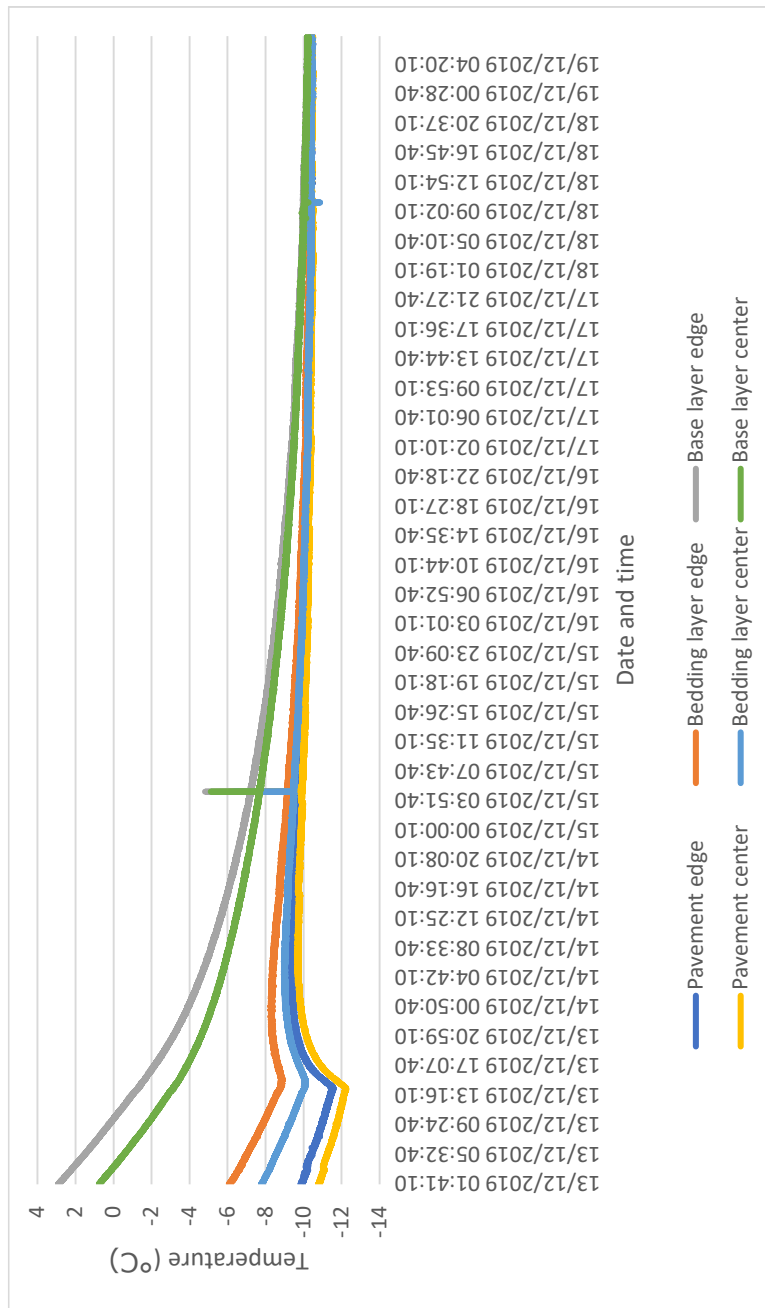


Figure 18: Temperature development in the pavement from 13/12/2019 until air temperature is turned up during pilot test 1.

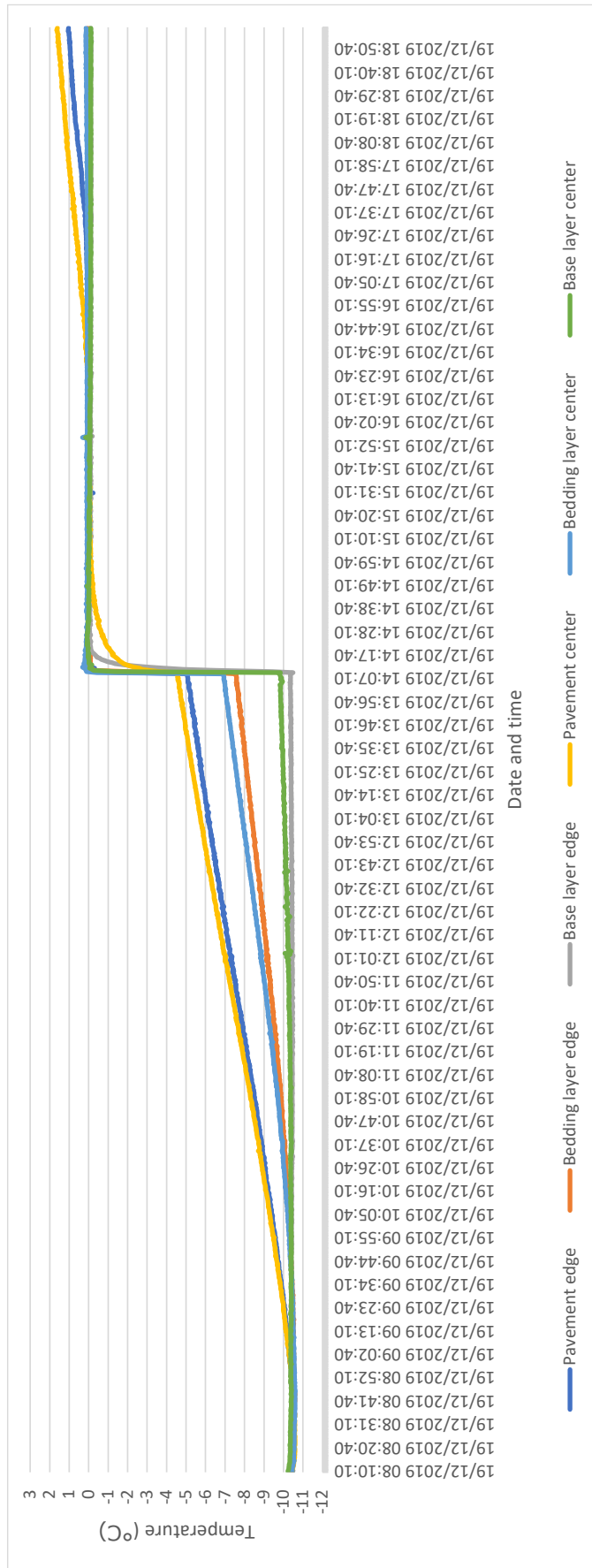


Figure 19: Temperature development in the pavement from the air temperature was turned up during pilot test 1.

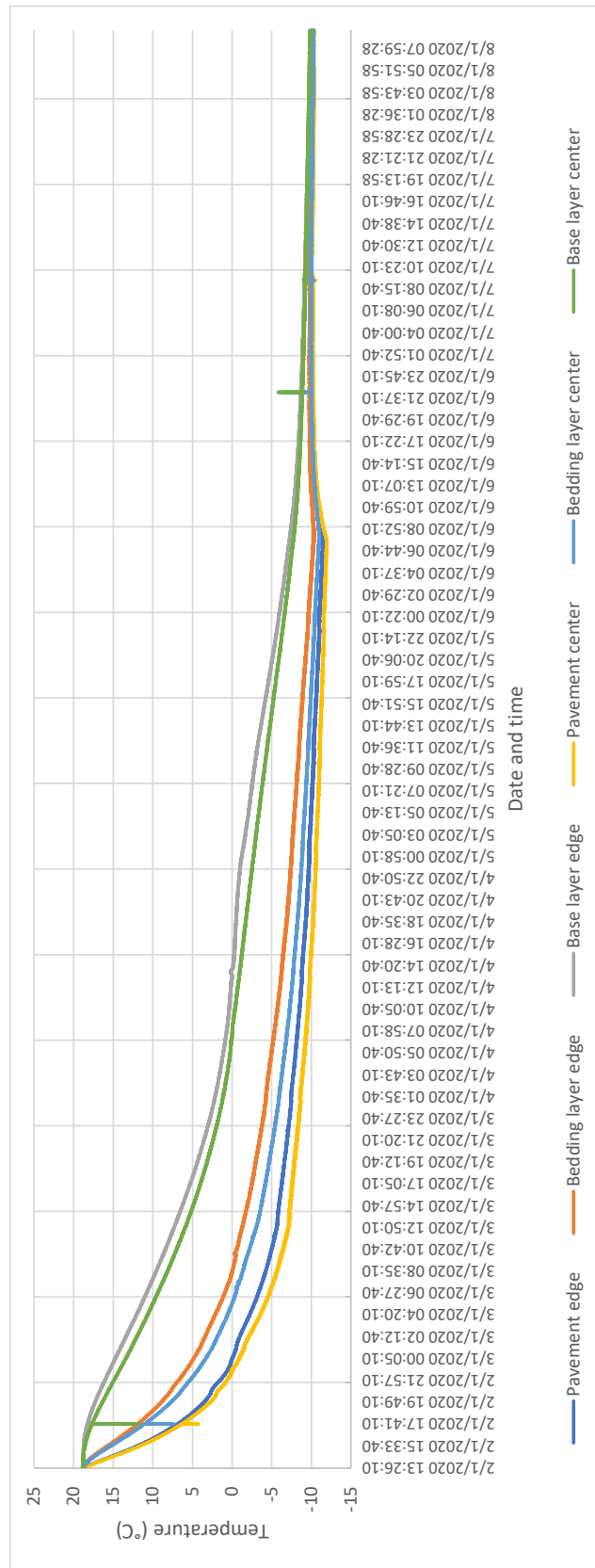


Figure 20: Temperature development in the pavement until air temperature is turned up during pilot test 2.

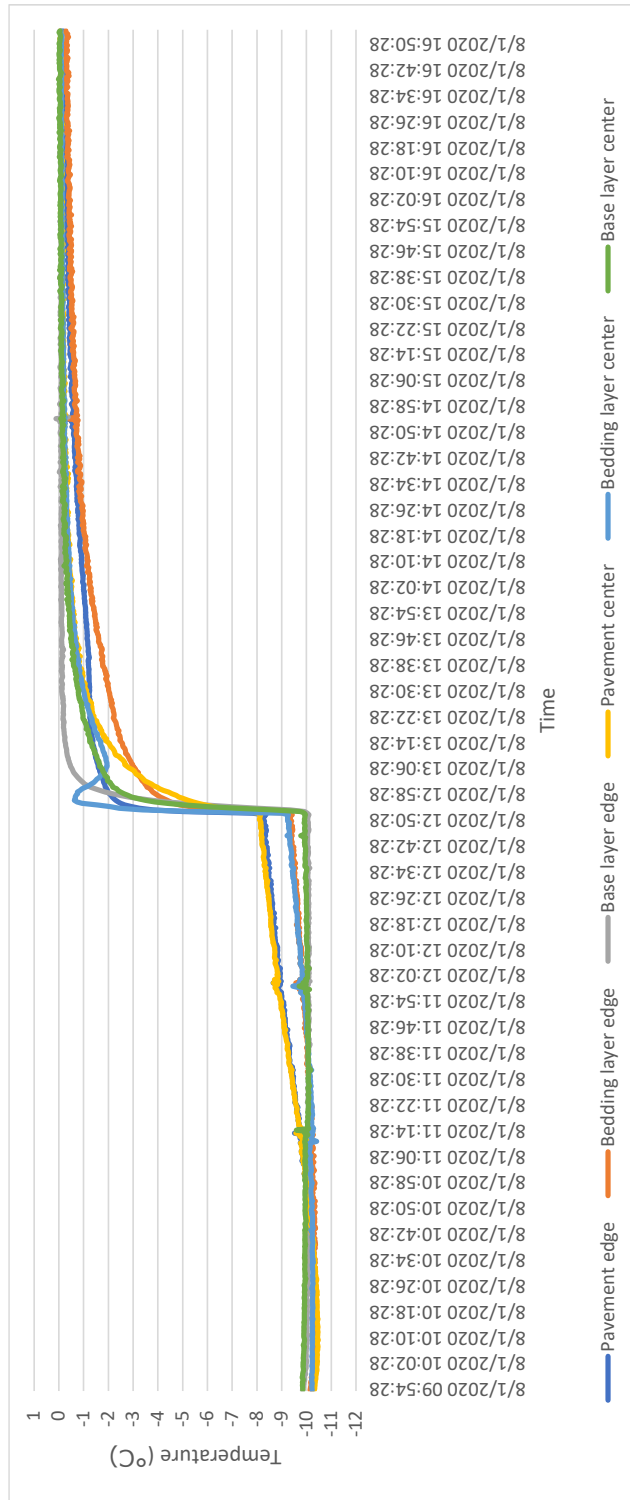


Figure 21: Temperature development in the pavement from the air temperature was turned up during pilot test 2.

